Proceedings of Meetings on Acoustics

Volume 19, 2013 http://acousticalsociety.org/

ICA 2013 Montreal
Montreal, Canada
2 - 7 June 2013

Musical Acoustics
Session 4aMU: Transient Phenomena in Wind Instruments: Experiments and Time Domain Modeling

4aMU8. Direct numerical simulations of the recorder in two and three dimensions

N Giordano*

***Corresponding author's address: Physics, Purdue University, 525 Northwestern Ave., West Lafayette, IN 47907, giordano@purdue.edu**

Direct numerical solutions of the compressible Navier-Stokes equations have been used to study various aspects of sound production in the recorder. A custom algorithm implemented on a parallel computer has enabled us to calculate tones and produce visualizations of the air flow near the labium in both two and three dimensions. In three dimensions we have observed how the attack portion of the tone and the spectrum at long times depends on the relative alignment of the channel and labium. We also describe subtle differences in the process of vortex shedding in two as compared to three dimensions.

Published by the Acoustical Society of America through the American Institute of Physics

Received 2 Jan 2013; published 2 Jun 2013

INTRODUCTION

The modeling of musical instruments continues to be of great interest. As computer power has steadily increased, the possibilities for ever more realistic modeling of various instruments has also increased. By "realistic modeling" we mean modeling that describes the essential elements of an instrument using fundamental physical laws. Much progress has been made in this area for instruments such as pianos and guitars, which requires solution of the equations of motion for strings and plates, along with the laws of linear acoustics (see, e.g., Giordano and Jiang [2004] and Bécache et al. [2005]). The modeling of wind instruments is more demanding since a first principles approach to modeling these instruments requires the application of the Navier-Stokes equations. Much progress has been made in understanding wind instruments through modeling that simplifies the problem in some way and avoids use of the Navier-Stokes equations; e.g., by making simplifying assumptions about the nature of the oscillations in the mouthpiece and the way these oscillations are coupled to a resonator. This type of modeling has given much insight into the operation of wind instruments, but there are questions that can only be dealt with by a first principles approach. Available computer power is now making it possible to numerically solve the Navier-Stokes equations for instruments such as the recorder, flue organ pipe, and flute. Indeed, several groups have demonstrated Navier-Stokes based simulations of these instruments in the past few years [Skordos 1995a, 1995b; Kühnelt 2003, 2004, 2005; Obikane 2009, 2010; Obikane and Kuwahara 2009; Miyamoto et al. 2010; Giordano 2013] and the field is now on the verge of using such simulations in quantitative studies of these instruments.

In this paper we describe a Navier-Stokes based study of the recorder in two and three dimensions. These computations require very substantial amounts of computer time, even when implemented on the fastest available high performance computers. The use of this approach to calculate musical tones in real time is not yet possible, but there are certain questions that can now be addressed with Navier-Stokes based modeling that are difficult or impossible to address in any other way. In this paper we describe a study of how the precise geometry of the flue channel affects the sound that is produced and show how relatively small changes in the design of the channel produce large changes in the attack portion of the tone. We also present results for the motion of the air jet as it exits the channel and impinges in the labium and compare the behavior found in two and three dimensional "instruments." The kind of modeling described here can be used to make predictions for channel and labium geometries that are not normally used in practical instruments and to devise new approaches to voicing recorders and related wind instruments.

METHOD

Many algorithms have been developed for solving the compressible Navier-Stokes equations. All of the results in this paper were obtained using the MacCormack method, a relatively straightforward algorithm that is known to work well for the regime of Reynolds, Mach, and Strouhal numbers encountered in a recorder [MacCormack 1969; MacCormack and Lomax 1979; MacCormack 1982]. This is an explicit predictor-corrector finite difference method that is second order accurate. We have applied the MacCormack method using the known speed of sound and kinematic viscosity of air (see Skordos [1995a] for a complete discussion of the equations). As found by previous workers, it was necessary to add a small amount of artificial viscosity to maintain numerical stability [Jameson et al. 1981; Swanson and Turkel 1987]. The effect of artificial viscosity is to suppress tubulent-like instabilities at length scales much smaller than those of physical interest. We have verified that the level of artificial viscosity used in our computations does not have any significant effect on the behavior at frequencies of musical interest.

The algorithm described here has been applied to model recorders in two and three dimensions, and the results are qualitatively similar. All of the results shown below were for a three dimensional recorder geometry like the one shown in Figure 1. (Some results for a two dimensional instrument are given elsewhere [Giordano 2013].) The recorder was placed in a virtual room with walls that reflected and absorbed sound as found in a typical room. The recorder was excited by imposing a flow velocity in the left hand portion of the channel. The smallest feature of the recorder was the height h of the channel, which was 1.0 mm. A nonuniform spatial grid was used with a spatial resolution inside and near the instrument of 0.1 mm in the vertical direction, 0.2 mm in the horizontal direction, and 1.0 mm in the direction perpendicular to the plane in Figure 1. Further details of the calculation and geometry are given in the caption of Figure 1 and elsewhere [Giordano 2013]. The recorder drawn in Figure 1 has a straight channel with the labium aligned with the center of the channel. We also explored the behavior with the labium aligned with the bottom of the channel and with a chamfered channel.

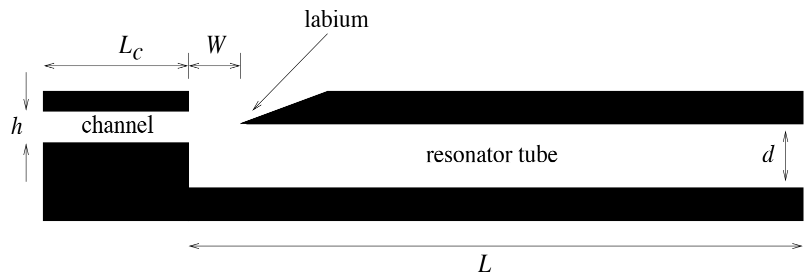

FIGURE 1. Recorder geometry. This is a cross-sectional view showing the plane that cuts through the center of the instrument. The resonator tube had a square cross-section with a channel width (in the direction perpendicular to the plane of this drawing) of 10.5 mm. The other dimensions were L_C = 8.0 mm, W = 4.0 mm, h = 1.0 mm, d = 10.5 mm, and L = 105 mm. The instrument was enclosed in a region of dimensions 0.2 x 0.06 x 0.06 m^3.

RESULTS

Dependence of the Spectrum on the Geometry of the Channel

The calculations yield the air density and velocity in and around the recorder as functions of time. The variation of the density with time is proportional to the acoustic pressure p, and Figure 2 shows the variation of p at a location at a point outside the recorder during the initial ("start-up") portion of a tone. Here the blowing speed in the left half of the channel was increased linearly from zero at $t = 0$ to its maximum value at $t = 5$ ms, and then held constant for the rest of the calculation (typically 50-100 ms). For the results in Figure 2 the blowing speed at the center of the channel was 30 m/s. The two recorder geometries considered in Figure 2 were identical except for the geometry of the channel. In (a) the recorder had a straight channel (as drawn in Figure 1) while in (b) the exit edges of the channel were chamfered. The chamfers were angled at 45º and the channel height at the exit was twice the height in the interior of the channel.

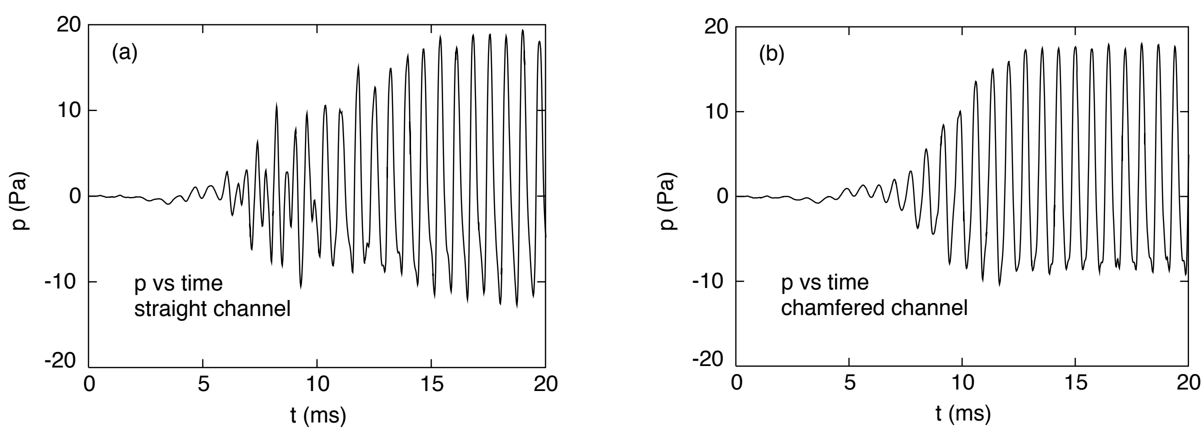

FIGURE 2. Sound pressure during the initial part of a tone as a function of time for two different channel geometries. (a) Left: A straight channel with the labium aligned with the center of the channel. (b) Right: A chamfered channel with the labium aligned with the center of the channel.

As noted above, the blowing speed was ramped up during the initial 5 ms. During this period the sound pressure increased very little, with the initial oscillations just beginning to become visible. For both channel geometries the sound amplitude increased rapidly after 5 ms, reaching a steady state by about 15 ms with the straight channel and about 13 ms with the chamfered channel. In both cases the steady state signal in the steady state was dominated by the component at the fundamental frequency, as found in real instruments. However, the behavior between 5 and 10 ms was quite different in the two cases. With the straight channel (Figure 2a) a component with a frequency higher than that of the fundamental is strong during this time, with that component becoming very small compared to the fundamental by about 12 ms. In contrast, with the chamfered channel (Figure 2b) the sound appears to be dominated by the fundamental component throughout.

Figure 3 shows spectra calculated using a Fourier transform analysis during the periods 5-10 ms, 10-15 ms, and 20-25 ms. The peaks here are somewhat broad due to the broadening inherent in the Fourier transform, but several features are clear. For the chamfered channel (Figure 3b) the spectra at all times are consistent with a sum of harmonic components, and the fundamental component dominates at all times, with the second, third and fourth harmonics being clearly visible. The spectra for the straight channel (Figure 3a) after 10 ms are similar, with the fundamental again being dominant. However, for the straight channel during the period 5-10 ms (Figure 3a, black curve) there is a strong inharmonic component that is approximately equal in amplitude to the fundamental. This inharmonic component has a frequency near 2300 Hz, which is much less than twice the fundamental frequency of about 1380 Hz and distinctly less than the second harmonic component at about 2750 Hz visible at longer times. Such inharmonic components during the attack portion of a tone have been reported in flue pipes by Castellengo [1999]; this appears to be the first observation of such behavior in modeling studies.

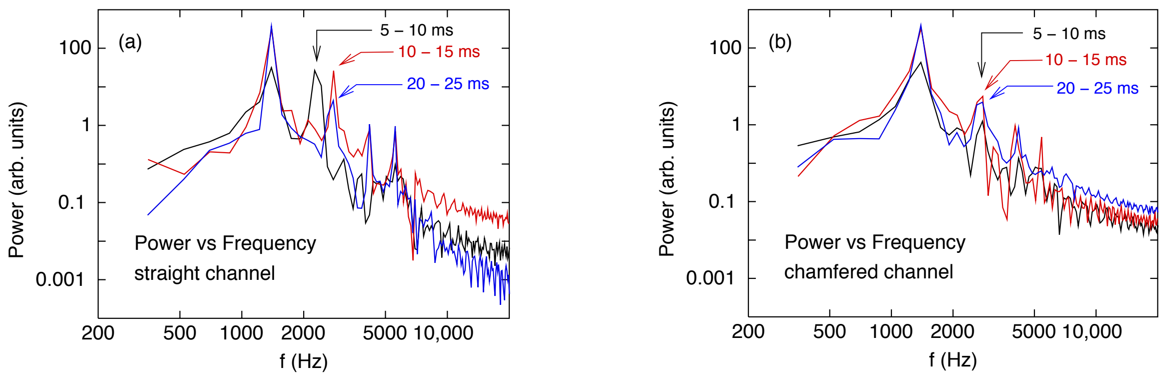

FIGURE 3. Spectrum during the initial part of a tone for three different time periods (5-10 ms / plotted in black, 10-15 ms / red, and 20-25 ms / blue) for (a) A straight channel with the labium aligned with the center of the channel, and (b) A chamfered channel with the labium aligned with the center of the channel.

Figure 4 shows how the two strongest components (the fundamental and the component at or near the second harmonic) vary with time. These results were obtained using short time Fourier transforms to determine the power for time windows of length 0.3 ms; other window lengths gave similar results. For the chamfered channel the power in the second harmonic is about two orders of magnitude less than the power at the fundamental frequency throughout most of the period shown, and is about a factor of 30 weaker at long times when the steady state tone is realized. In contrast, for the straight channel the strength in the frequency range encompassing both the inharmonic component observed in Figure 3a and the second harmonic is as strong as the fundamental between about 6 and 9 ms, confirming what is evident by eye in Figure 2a. These results demonstrate that the attack portion of the recorder tone is a very strong function of the channel geometry, as observed in experimental work on recorder-like geometries [Ségoufin et al. 2000] and flue organ pipes [Castellengo 1999].

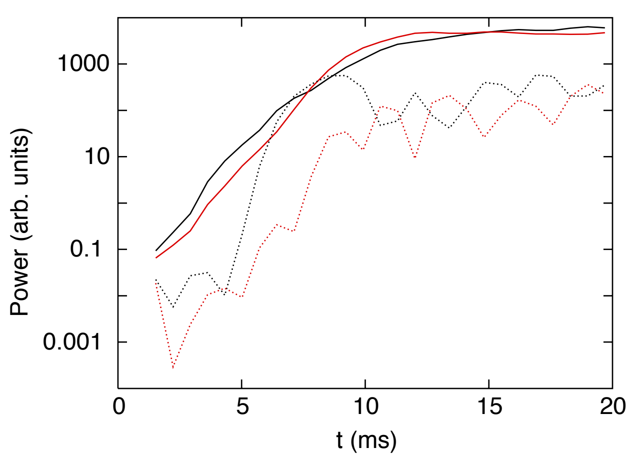

FIGURE 4. Solid lines: Power at the fundamental frequency as a function of time. Dotted lines: Power in the frequency range near the second harmonic (and including the inharmonic component observed in Figure 3a) as a function of time. The different

colors denote results for the different channel geometries, with black denoting results for the straight channel and red denoting results for the chamfered channel.

Dynamics of the Air Jet

Detailed insight into the behavior of the instrument can also be gained by examination of the air jet as it leaves the channel and impinges on the labium. This kind of information is readily accessible with Navier-Stokes based modeling, and can also be obtained by experiments through schlieren photography (see, e.g., Fabre et al. [1996]). Figure 5 shows results for the motion of the air jet for the straight channel geometry. The images in Figure 5 span approximately one cycle of oscillation at the fundamental frequency and were recorded in the steady state region of Figure 2. These images show only the region very near the channel exit and labium, and show the behavior on a plane parallel to the plane of Figure 1 and cutting through the center of the channel. The air jet is seen to oscillate up and down relative to the labium; these oscillations and the associated pressure oscillations are the source of the sound produced by the instrument. The behavior of the air jet in three dimensions seen in Figure 5 differs from that found in two dimensional simulations [Giordano 2013]; in two dimensions the center of the air jet was found to stay at or above the bottom of the labium at all times. This suggests that simulation studies of the recorder and related instruments will be most useful when they employ a three dimensional geometry.

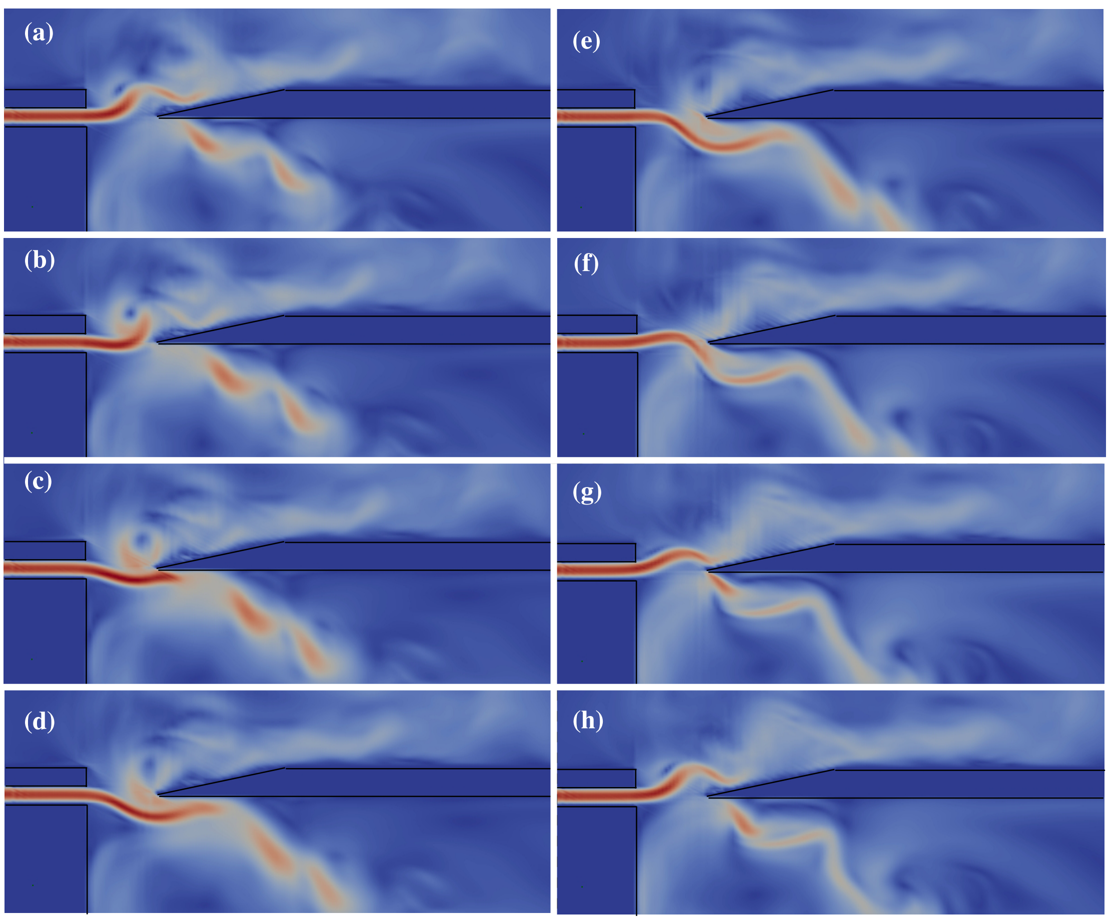

FIGURE 5. Images of the air jet for the case of a straight channel. These are expanded views of the region near the exit of the channel. The edges of the channel and labium are indicated with black lines; the full simulation region is much larger than shown here. The dark red color indicates a high air speed while dark blue regions are places of very low speed. These images show the speed on a plane that cuts through the center of the recorder, corresponding to the plane of the drawing in Figure 1. Images (a)-(h) show how the air jet varies during the course of one oscillation period, which was approximately 0.71 ms. These images were obtained after t = 50 ms in the simulation shown in Figure 2a. Note that the height of the channel was 1.0 mm and the distance from the exit of the channel to the sharp edge of the labium was 4.0 mm.

The images in Figure 5 are qualitatively very similar to those reported in experiments (e.g., Fabre et al. [1996]). It should be possible to carry out simulations for geometries that precisely match the experiments and make quantitative comparisons. It is worth noting that one must be careful when comparing the results in Figure 5 with experiments, since the experimental images typically produce an average over the entire width of the channel in the direction perpendicular to the plane in Figure 1. Our simulations contain full information on the velocity field throughout the regions visible to the experiments, and this information can be used to calculate images that correspond to what is measured in the experimentally. We have examined images of the air jet close to the side wall of the channel and resonator tube, and those images differ in subtle but significant ways from images obtained from the center of the channel. This is a problem that we will report on in the future.

DISCUSSION

This paper presents results of a modeling study of a recorder in three dimensions using the Navier-Stokes equations. Our results show that the harmonic content during the initial portions of the tone is very sensitive to the geometry of the channel. The behavior we observe for a straight channel is qualitatively similar to that observed for recorders [Ségoufin et al. 2000] and flue organ pipes [Nolle 1979; Nolle and Finch 1992; Castellengo 1999]. (See Fletcher [1976] for a discussion of theoretical aspects of this problem.) In addition, our results show that adding chamfers to the channel changes the initial harmonic content dramatically, as the large inharmonic component found for a straight channel is greatly suppressed with a chamfered channel. This appears to also be in good agreement with experiments, and shows that our modeling is able to accurately capture the effect of relatively small changes in instrument geometry. This also suggests that modeling of the kind described here should be a useful way to explore how other possible changes in this class of instruments will affect their musical tones.

ACKNOWLEDGMENTS

I thank D. M. Roudebush for providing sound spectra for several real recorders, and the Rosen Center for Advanced Computing at Purdue University for access to the computational resources essential for this work.

REFERENCES

Bécache, E., Chaigne, A., G. Derveaux G. and Joly, P. **(2005)**. "Numerical simulation of a guitar," Computers and Structures **83**, 107–126.

Castellengo, M. **(1999)**. "Acoustical analysis of initial transients in flute like instruments," Acustica-acta acoustica **85**, 388-400.

Fabre, B., Hirschberg, A. and A. P. J. Wijnands, A. P. J. **(1996)**. "Vortex shedding in steady oscillaion of a flue organ pipe," Acustica **82**, 863–877.

Fletcher, N. H. **(1976)**. "Transients in the speech of organ flue pipes - a theoretical study," Acustica **34**, 224-233.

Giordano, N. **(2013)**. "Direct numerical simulation of a recorder," J. Acoust. Soc. Amer. (in press).

Giordano, N. and Jiang, M. **(2004)**. "Physical modeling of the piano," European Journal of Applied Signal Processing, special issue **2004-7**, 926-933.

Jameson, A., Schmidt, W. and Turkel E. **(1981)**. "Numerical solution of the Euler equations by finite volume methods using Runge-Kutta time stepping schemes," AAIA Paper **81**-1289, 1–14.

Kühnelt, H. **(2003)**. "Simulating the mechanism of sound generation in flutes using the lattice Boltzmann method," in *Proceedings of the Stockholm Music Acoustics Conference (SMAC03)*, SMAC1–SMAC4.

Kühnelt, H. **(2004)**. "Simulating the mechanism of sound generation in flutes and flue pipes with the lattice-Boltzmann-method," in *Proceedings of the International Symposium on Musical Acoustics, Nara, Japan*, 251–254.

Kühnelt, H. **(2005)**. "Simulation and analysis of the flow-acoustic interactions in the mouth of flute-like instruments," in *Forum Acusticum (European Conference on Acoustics) Budapest*, 1–6.

MacCormack, R. W. **(1969)**. "The effect of viscosity in hypervelocity impact cratering," AAIA Paper **69**-354 1–7.

MacCormack, R. W. and Lomax, H. **(1979)**. "Numerical solution of compressible viscous flows," Ann. Rev. Fluid Mech. **11**, 289–316.

MacCormack, R. W. **(1982)**. "A numerical method for solving the equations of compressible viscous flow," AIAA Journal **20**, 1275–1281.

Miyamoto, M., Ito, Y., Takahashi, K., Takami, T., Kobayashi, T., Nishida, A. and Aoyagi, M. **(2010)**. "Applicability of compressible LES to reproduction of sound vibration of an air-reed instrument," in *Proceedings of the International Symposium on Musical Acoustics,* Sydney and Katoomba, Australia, 1-10.

Nolle, A. W. **(1979)**. "Some voicing adjustments of flue organ pipes," J. Acoust. Soc. Amer. **66**, 1612-1626.

Nolle, A. W. and T. L. Finch **(1992)**. "Starting transients of flue organ pipes in relation to pressure rise time," J. Acoust. Soc.

Amer. **91**, 2190-2202.

Obikane, Y. **(2009)**.“Direct simulation on a fipple flute using the compressible Navier-Stokes equation,” World Academy of Science, Engineering and Technology **4**, 794–798.

Obikane, Y. **(2010)**.“Computational aeroacoustics on a small flute using a direct simulation,” in *Computational Fluid Dynamics 2010*, edited by A. Kuzmin, 435–441 (Springer-Verlag, New York).

Obikane, Y. and Kuwahara, K. **(2009)**.“Direct simulation for acoustic near fields using the compressible Navier-Stokes equation,” Computational Fluid Dynamics **2008/2009** 85–91.

Ségoufin, C., Fabre, B., Verge, M. P., Hirschberg, A. and Wijnands, A. P. J. **(2000)**. “Experimental study of the influence of the mouth geometry on sound production in a recorder-like instrument: Windway length and chamfers,” Acustica-acta acustica **86**, 649-661.

Skordos, P. A. **(1995a).** *Modeling of flue pipes: Subsonic flow, lattice Boltzmann and parallel distributed distributed computers*, Ph.D. thesis, MIT.

Skordos, P. A. and Sussman G. J. **(1995b).** “Comparison between subsonic flow simulation and physical measurements of flue pipes,” in *Proceedings of the International Symposium on Musical Acoustics, Dourdan, France*, 1–6.

Swanson, R. C. and Turkel, E. **(1987)**. “Artificial dissipation and central difference schemes for the Euler and Navier-Stokes equations,” AIAA paper **87**-1107, 55-69.